6. STABILIZATION OF THE APNS BY COORDINATED POWER SYSTEM STABILIZERS

6.1 Introduction

Control laws utilized to achieve stability enhancement can be divided into two classes: continuous and non-continuous. Continuous control methods are the primary controls, i.e., controls by speed governor, excitation system and power system stabilizer. They are very well understood and documented [27,28,29]. More detailed investigation of their applications in the APNS is reported in this chapter.

Non-continuous control methods are corrective remedies used to achieve stable operations without expensive network reinforcement. These corrective measures are called discrete supplementary controls. There are several such control schemes [34] and each can provide a particular control effect. For a specific application in a practical power system, not all of them can be employed. As far as the APNS is concerned, only hydro plants exist and they are far away from the load center. The total generation capacity is small and running voltage is not high. Reinforcement of the very long transmission lines is costly and is unrealistic. Load flow studies reported in Chapter 4 indicate that a large power imbalance exists in all the three geographically divided areas. Taking all these factors into account, the following two corrective measures may be considered as appropriate to be employed in the APNS to improve its overall system stability: (a) generator tripping and (b) load shedding.

An appropriate application of these two methods must meet the practical requirement of the system operation and customers' demands. As this information is not available to the author at this moment, only continuous control methods were considered in the study reported in this thesis.

As shown in Chapter 4, the common practice to provide positive damping through excitation control is to use PSSs. Usually, the system modes must be known in PSS design. It is also generally true that the damping (real part) of a system mode is more sensitive to operating conditions than the frequency (imaginary part) of that mode. Reduction of these sensitivities of a mode increases the robustness of the PSS designed based on this mode. In this thesis, instead of using a specific frequency for a particular PSS design, an average frequency is derived for each coherent group of generators that oscillate together. The coherent generation groups can be identified by available methods [32]. Another parameter needed in tuning the PSS is a lead/lag time constant spread [25,26]. Nonlinear simulation is utilized to determine the optimum gain of each PSS. The last step is to coordinate the application of the designed PSSs. Input signals to all the PSSs in each coherent generation group are to be communicated with each other between two strongly coupled generators. The total coupling factors [33] computed from eigenanalysis are employed to take into account these interactions among generators.

6.2 Effect of Existing Primary Controls

The effect of the automatic voltage regulator (AVR) on dynamic stability has been discussed in Chapter 4 by eigenvalue analysis and computing parametric and functional sensitivities. There the effects of speed governors and power system stabilizers have been intentionally neglected as their effects are inappreciably small. These observations are further illustrated in this section by time simulation under a specific disturbance.

6.2.1 AVR Effect

In order to illustrate the effect of the AVR, it was chosen to fix all other parameters of the available controllers in the system and change only the AVR gain and its time constant, respectively.

Time domain simulations for three situations were carried out. Specifically, they are:

a). when the gain K_A of each AVR was set to be 0.001, i.e., the AVR is disabled;

b). when the gain K_A of each AVR was set to be its existing value; and

c). when the time constant T_A of the regulator of each AVR was set to be a large value, i.e., 10 seconds.

Figures 6.1 and 6.2 show typical responses of the rotor angle and terminal voltage of generator #8 for each of the three situations. The following observations can be made:

1). When the time constant of the AVR is large, the oscillation of the rotor angle is depressed and better damped, as per Figure 6.1.

2). When the AVRs are disabled by setting their gains very small, the terminal voltage can be quickly restored to normal value after the fault clearing, while the oscillation of the rotor angle is much more severe, especially the first swing, as per Figures 6.1 and 6.2. This is because that the field voltage of the machine does not increase and therefore the output electrical power can not be raised. Hence the net accelerating power is large.

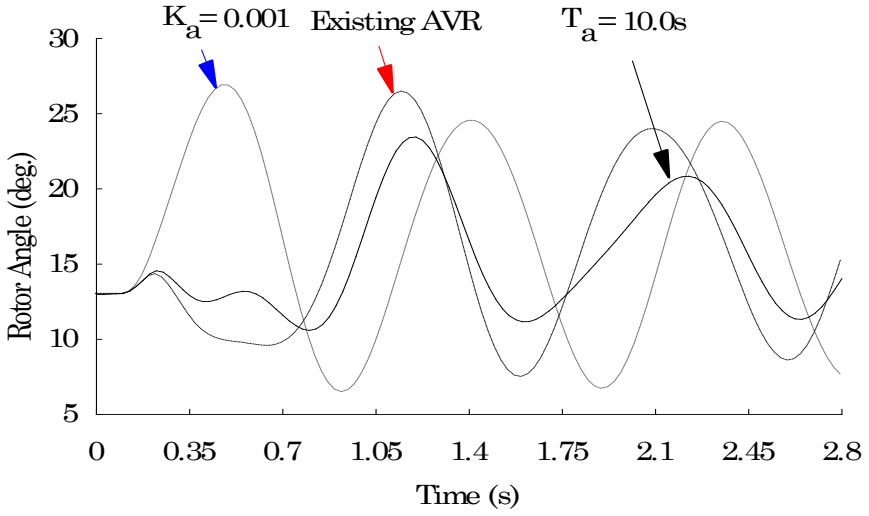

Figure 6.1: Rotor angle plotting of generator #8 under 3ϕ fault at bus 30.

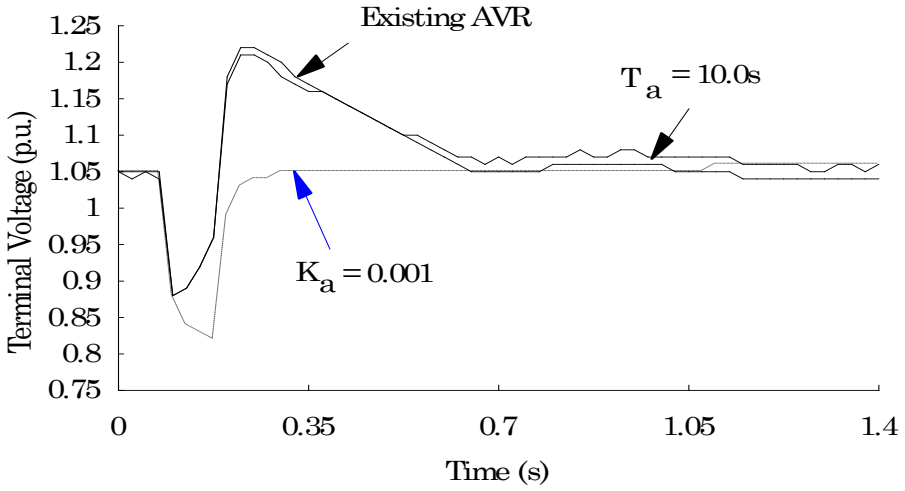

Figure 6.2: Terminal voltage plotting of generator #8 under 3ϕ fault at bus 30.

6.2.2 Speed Governor Effect

As explained in Chapter 2, the speed governing and turbine system (SGTS) of a hydro generator can be simulated by either the accurate model or the approximate model.

In the APNS, the SGTS for generators #8 to #12 was simulated by the accurate model. The various parameters used in the model are in their normal ranges. The SGTS for generators #1 to #7 was simulated by the simplified model. The time constant T_1 of generator #1 to #3 is 33.15 seconds and that of generators #4 to #7 is 51.2 seconds. Figure 6.3 illustrates the mechanical power responses of generator #1 when the time constant T_1 changes from 33.15s to 3.315s. It can be seen that when the time constant T_1 of generator #1 was set to 3.315s, one tenth of the existing value, the change of mechanical power was about nine times larger, as shown in Figure 6.3.

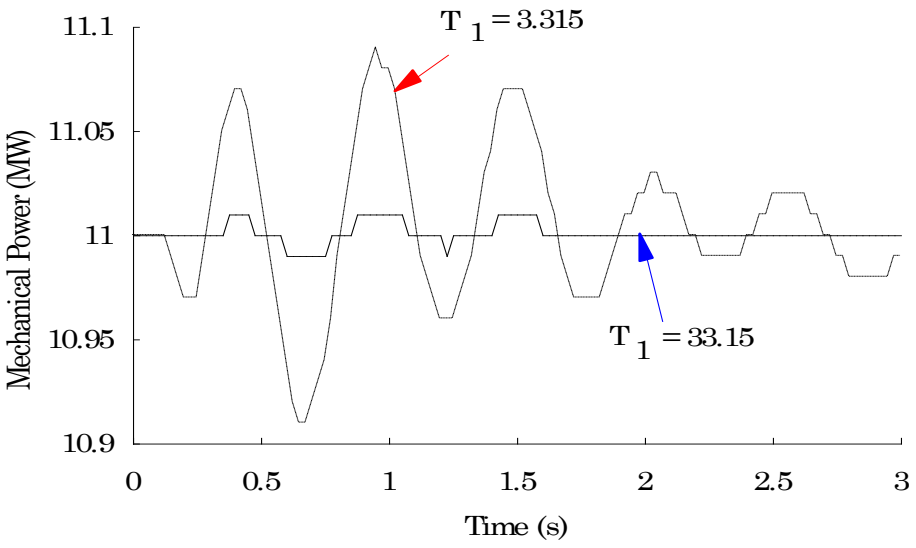

Figure 6.3: Mechanical power of generator #1 under 3ϕ fault at bus 30.

6.2.3 PSS Effect

Generators #1 through #7 are equipped with PSSs which uses generated electrical power as input signal. The transfer function of the PSS has the form as given in (6.1):

$$G_{pss}(s) = K\left(\frac{1+sT_1}{1+sT_2}\right)\left(\frac{T_3 s}{1+sT_4}\right)\left(\frac{sT_5}{1+sT_6}\right)\left(\frac{1}{1+sA_1}\right) \tag{6.1}$$

The values of the parameters in the transfer function are given in Table 2.1. The output of the PSS under disturbances is negligibly small, as shown in Figure 5.5 in Chapter 5. It is believed that utilization of more effective PSSs would be beneficial.

Generators #8 and #9 are equipped with PSS using accelerating power as input signal. The transfer function of the PSS has the form as given in (6.2):

$$G_{pss}(s) = K\left(\frac{1+sT_1}{1+sT_2}\right)\left(\frac{1+sT_3}{1+sT_4}\right)\left(\frac{sT_5}{1+sT_6}\right) \tag{6.2}$$

The actual parameters in the transfer function are also given in Table 2.1 of Chapter 2. Figure 6.4 illustrates the differences of rotor angle responses of generators #1 and #8 for a 3ϕ fault at bus 30 with and without the existing PSSs in the system. It can be seen that the PSS on generator #8 has a slightly greater impact on oscillation than that on generator #1. On the other hand, the oscillation of generator #1 is less severe than that of generator #8, as the former is closer to the infinite busbar. It is possible to design more effective PSSs for the system to improve its overall stability. More discussion of this topic is presented in the following section.

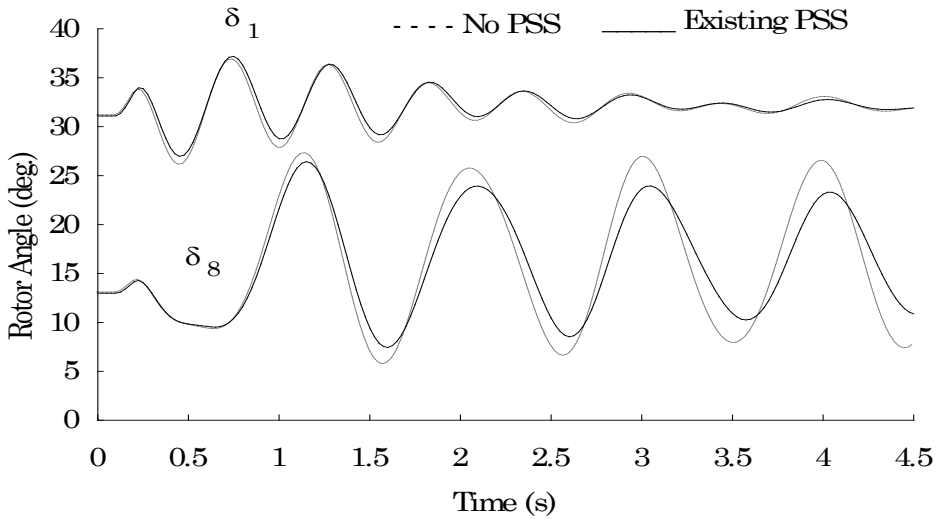

Figure 6.4: Rotor angle swing of generators #1 and #8 under 3 ϕ fault at bus 30. Effects of PSSs.

6.3 Coordinated PSS Design

As has been explained in Chapter 3, power system stabilizers (PSSs) have been widely utilized in excitation control to provide positive damping. In most conventional PSS applications, only local feedback control is used. A multivariable and/or optimal stabilizer can be designed theoretically but may not be implemented because of the difficulties in accurately obtaining required controlling inputs. Coordination in PSS design has been considered by either eigenanalysis [35], or frequency domain methods [36] or a hybrid of the two [37]. No matter what algorithm is employed in tuning the settings of a PSS, the more information dependent on operating conditions is used, the less robust the PSS will be to system changes.

A new coordinated PSS design procedure is proposed in this thesis. It is based on generation coherency, the total coupling factors and non-linear simulation.

6.3.1 Design Procedure

According to the previous analysis, the negatively damped modes λ_1,λ_2,λ_6,λ_8 to λ_{12} mainly involve generators #1 to #10. In order to provide positive damping, these generators have been actually equipped with PSSs with the exception of generator #10. This chapter attempts to utilize different but very effective PSSs to further enhance the dynamic and transient stability of the system.

To design a PSS, it is essential to choose a proper input signal and then design a compensation circuit reasonably robust to different operating conditions. Because of the interactions among generators, there seems to be

no way to correspond each and every swing mode with one specific machine. A coordinated design and application procedure for PSSs was developed during the research reported in this thesis. The procedure is outlined below:

- Determine the coherent generation groups by an available technique [32].
- Find the average center frequency for each group of generators participating in various swing modes together.
- Choose a PSS input, say shaft speed.
- Let the system operate at full load and the strongest transmission for speed input type PSS tuning.
- Set a washout time constant.
- Set a lead/lag time constant spread for the compensation circuit of the PSS.
- Determine the time constants according to the center frequency and the spread.
- Change the PSS gain from 0 to infinity and compute the root loci or perform non-linear time simulations. When instability is met, the best gain value is chosen to be one third of the gain at instability [25].
- Evaluate the effectiveness of the settings by either eigenvalue analysis or time domain simulations. Change the spread if necessary and repeat the last three steps.

6.3.2 PSS Tuning

Extensive time simulations and calculations of coupling factors have shown that the following coherent generator groups can be identified: (#1,#2,#3,#7), (#4,#5,#6), (#8,#9) and (#10,#11,#12). The tuning of PSSs for generator group 1 is illustrated here. It is shown in Table 3.2 that the generators in group 1 participate in various swing modes at an average frequency of 1.9 Hz. The system is assumed to be operating at full load with the network intact. The time constant spread is set to be 8:1 and the deviation of the generator shaft speed with respect to the synchronous speed is chosen as the PSS input. The transfer function of a speed input PSS is given by:

$$G_{pss}(s) = K_s \left(\frac{T_w s}{1+T_w s} \right) \left(\frac{1+T_1 s}{1+T_2 s} \right) \left(\frac{1+T_3 s}{1+T_4 s} \right) \tag{6.3}$$

The initial lead/lag time constants, T_1,T_2,T_3 and T_4 are determined as follows [25]:

$$T_1 = T_3 = \sqrt{8} / 2\pi f_c = 0.237\text{s} \tag{6.4}$$

$$T_2 = T_4 = T_1 / 8 = 0.03\text{s} \tag{6.5}$$

where f_c is the average (or central) oscillation frequency of generation group 1. The gain K_s is set to be equal to 5 and the washout time constant T_w is 10s. The final settings after adjustments are listed in Table 6.1. PSSs for other generation groups were also designed and their settings are also listed in Table 6.1.

Table 6.1: PSS settings of the 4 generation groups

Group No	Ks	T1/T2	T3/T4	Tw
1	5	.2465/.0342	.2465/.0342	10
2	5	.2350/.0290	.2350/.0290	10
3	10	.2000/.0100	.1000/.0300	6
4	10	.2000/.0100	.1000/.0300	6

6.3.3 Communication of PSS Inputs

In order to increase the robustness of single input PSSs and to reflect the coupling among generators, the stabilizer inputs in each group will be communicated among its PSSs. As all the generators in a coherent group behave in a very similar fashion, their speed deviations with respect to the synchronous speed will be either positive or negative. These speed deviations can be summed up through the coupling factors to feed each PSS in that group as illustrated in Figure 6.5.

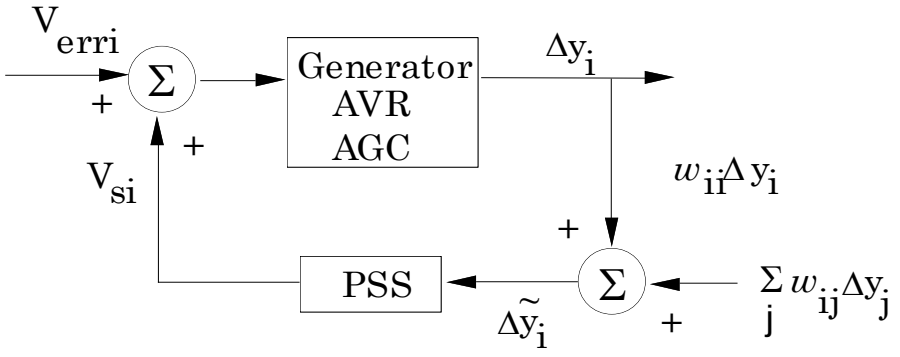

Figure 6.5: Realization of PSS coordination.

Fortunately, the generators in each group of the first three groups are in the same plant and the last group involves two plants seven kilometers away.

Therefore, only local communication is required, which can be realized without difficulty.

The input signal to the i-th PSS is given by:

$$\Delta\tilde{y}_i = w_{ii}\,\Delta y_i + \sum_{j\neq i} w_{ij}\,\Delta y_j = \sum_{j} w_{ij}\,\Delta y_j \tag{6.6}$$

where w_{ij} is the total coupling factor between generator i and generator j computed from eigenvalue analysis and reflects the extent of interaction between the two generators, and Δy_j is a measurable output of the j-th plant. For a speed input PSS, Δy_j is the speed deviation of generator j. The coupling factors calculated from eigenvalue analysis are listed in Table 6.2. Values less than 10^{-2} are neglected.

Table 6.2: Total coupling factors w_{ij}

Gen No	1	2	3	4	5	6	7	8	9	10	11	12
1	0.33	0.13	0.08	0.02	0.02	0.02	0.05	0	0	0	0	0
2	0.13	0.2	0.21	0.02	0.02	0.02	0.05	0	0	0	0	0
3	0.08	0.21	0.25	0.02	0.02	0.02	0.05	0	0	0	0	0
4	0.02	0.02	0.02	0.18	0.06	0.06	0.01	0	0	0	0	0
5	0.02	0.02	0.02	0.06	0.12	0.12	0.01	0	0	0	0	0
6	0.02	0.02	0.02	0.06	0.12	0.12	0.01	0	0	0	0	0
7	0.05	0.05	0.05	0.01	0.01	0.01	0.23	0	0	0	0	0
8	0	0	0	0	0	0	0	0.45	0.45	0.09	0.22	0.44
9	0	0	0	0	0	0	0	0.45	0.45	0.09	0.22	0.43
10	0	0	0	0	0	0	0	0.09	0.09	0.33	0.67	0.26
11	0	0	0	0	0	0	0	0.22	0.22	0.67	3.85	2.07
12	0	0	0	0	0	0	0	0.44	0.43	0.26	2.07	3.43

6.4 Improvement of System Stability by New PSSs

It is expected that the new PSSs should be able to provide positive damping to various swing modes once they are installed in the system. Eigenvalue analysis and time simulations were performed in this section with the new PSSs in service.

6.4.1 New Eigenvalues

Eigenvalue analysis of the system with these newly designed PSSs in service was performed and the results are listed in Table 6.3. It can be seen in Table 6.3 that the above designed PSSs are very effective in providing positive damping to almost all swing modes when they are installed on generators #1 to #7. It can also be seen that swing modes λ_1 and λ_9 are still slightly negatively damped. When new PSSs are also installed on generators #8 and #9, these swing modes will also become positively damped.

6.4.2 Time Simulation of the Small Disturbance

The small disturbance previously studied in Section 4.6 was simulated with new PSSs on generators #1 - #9 without coordination. Figure 6.6 illustrates the rotor angle swing of generators #1 and #8. The oscillations are damped out in 5 seconds. This is a significant improvement as compared to the situation presented in Figure 4.5 where the existing PSSs were in service.

Table 6.3: Eigenvalues after installation of new PSS on #1-#7

Swing No	σ	ω	freq. (Hz)
1	0.060	5.919	0.90

2	-2.727	6.748	1.16
3	-2.853	6.851	1.18
4	-0.686	7.233	1.15
5	-2.836	7.514	1.28
6	-4.215	8.505	1.44
7	-2.950	8.942	1.5
8	-4.395	9.412	1.59
9	0.010	10.865	1.74
10	-0.042	11.107	1.75
11	-0.067	11.728	1.88
12	-0.054	12.268	1.95

6.4.3 Time Simulation of a Large Disturbance

As a demonstration of the function of the new PSSs when installed in the system and a verification of their effectiveness, a single phase to ground (SLG) fault on the double circuit line 59-61 near to bus 61 for 6 cycles was simulated. It was cleared by opening all the three phases of the faulted line. Figure 6.7 shows the rotor angle swings of generator #1 with the existing PSSs on generators #1 to #9 and new PSSs on generators #1 to #7, respectively. It is clearly shown that new PSSs can effectively damp down the oscillations and enhance system stability. Detailed comparison is provided in the next section.

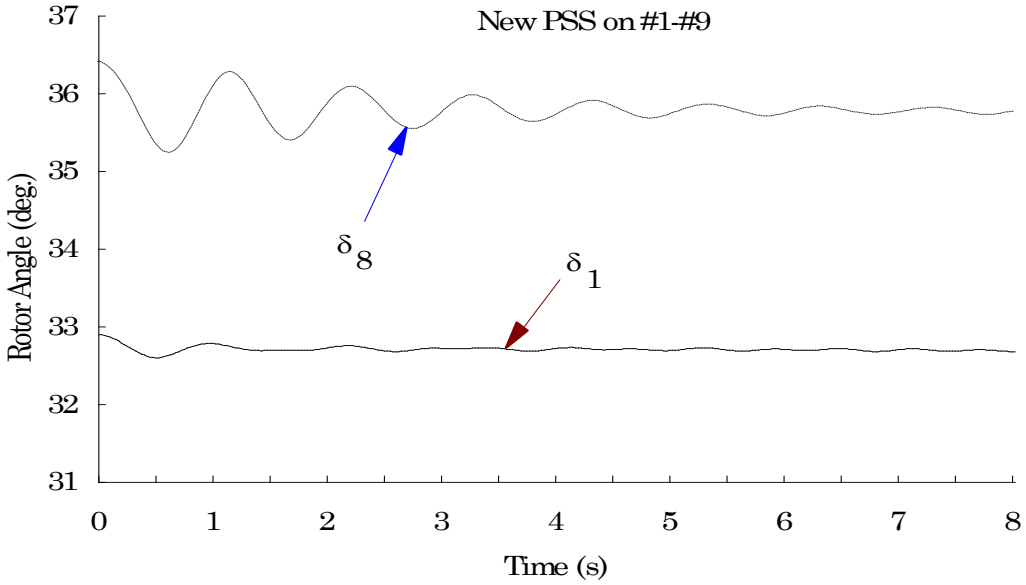

Figure 6.6: Rotor angle swing responding to a load increase of 1% the system capacity at Rabbit Lake.

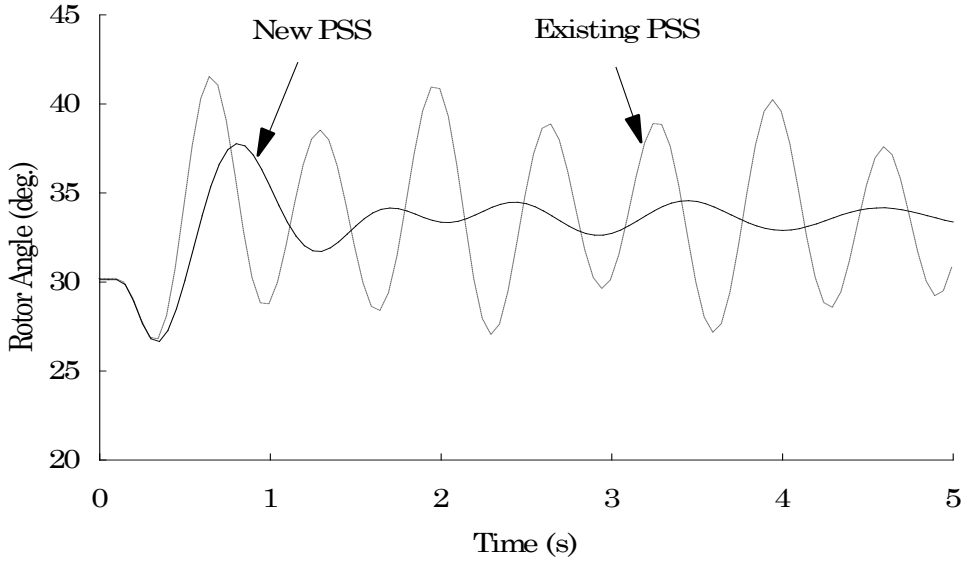

Figure 6.7: Rotor angle plotting of generator #1 versus time. Single phase fault near bus 61 for 6 cycles.

6.5 Transient Simulation Studies

Considering the actual difficulties in implementation of power system stabilizers at generators #10 to #12 because of their rotating excitation systems and in provision of extra communication means between these two plants, the application of the new PSSs was divided into two stages. Stage I: only generators #1 to #9 were equipped with new PSSs. Stage II: the remaining three generators were also equipped with PSSs. The two disturbances, i.e., the (SLG) fault and the 1% load increase at Rabbit Lake covered in Chapter 4, were employed for simulation studies. Other simulation tests are also included.

6.5.1 Existing PSSs

Simulations were conducted with and without the existing PSSs on machines #1 to #9 for the single phase to ground (SLG) fault condition. Figure 6.8(a) shows that the system was unstable if no PSS was installed in the system. When the existing PSSs were put into service, the system stability was improved significantly, as seen in Figure 6.8(b). Figure 6.8(c) displays the outputs of the existing PSSs.

6.5.2 New PSS on #1-#9

When the new PSSs are installed on generators #1 to #9, the sustained oscillations can be damped out much quicker in Figure 6.9(a), as compared with Figure 6.8(b). Further improvement in damping is also illustrated when coordination is incorporated in Figure 6.9(b). The outputs of new PSSs on generators #1 and #8 are given in Figure 6.9(c).

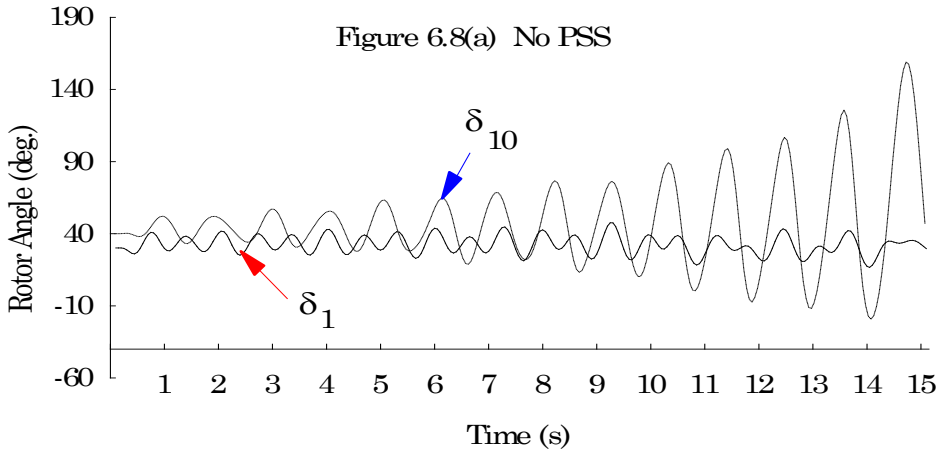

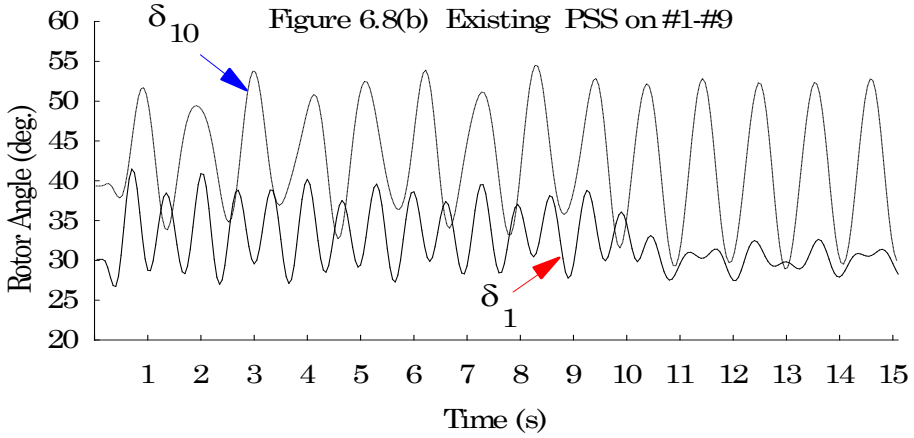

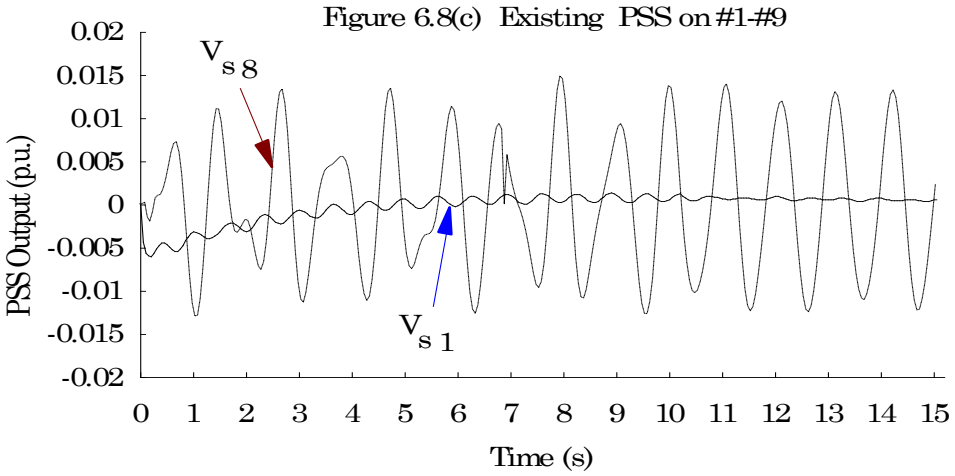

Figure 6.8: Time domain simulation of the SLG fault with and without the existing PSSs in service.

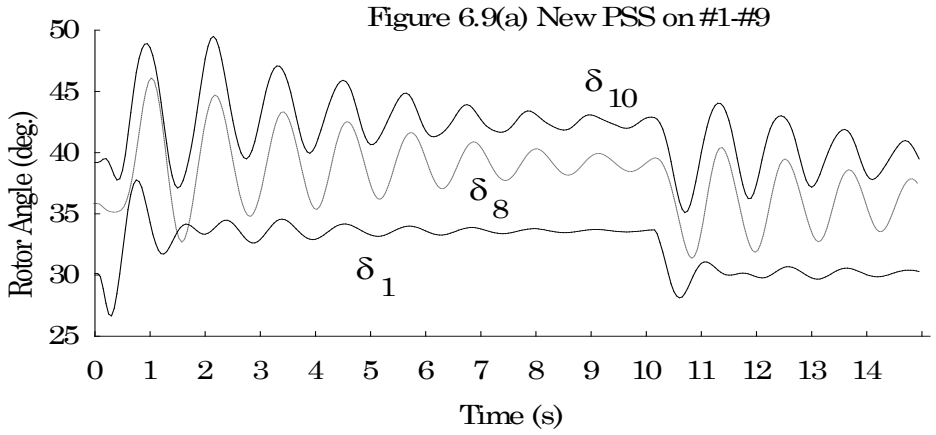

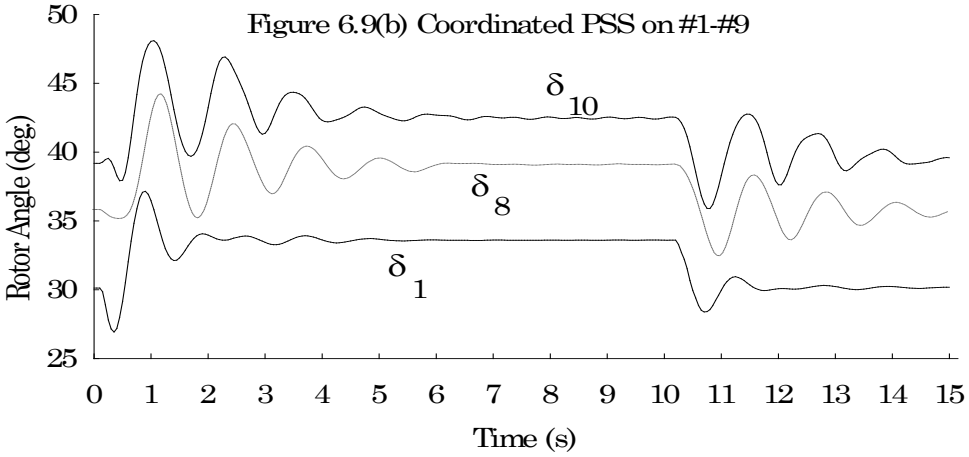

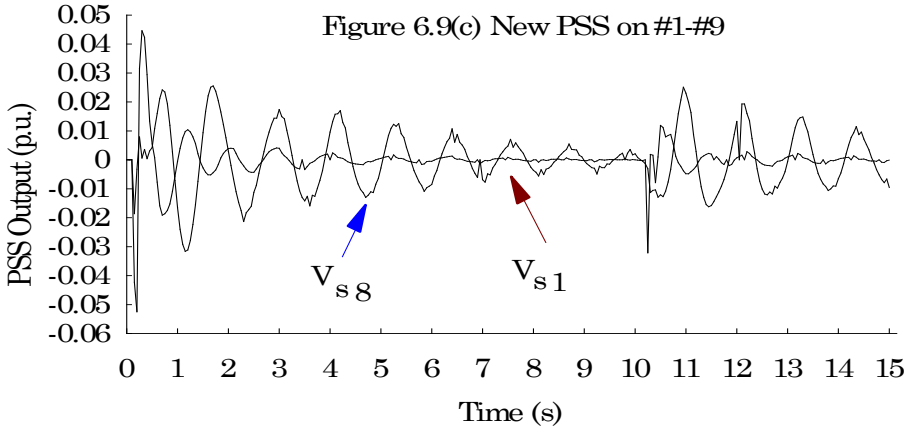

Figure 6.9: Time domain simulation of the SLG fault with new PSSs on generators #1 - #9 in service.

6.5.3 New PSSs on All Machines

If the three hydro generators of the last coherent generation group are also equipped with new PSSs, further enhancement in dynamic and transient stability can be expected. This is illustrated in Figure 6.10(a) and 6.10(b). The latter is with coordinated PSS application.

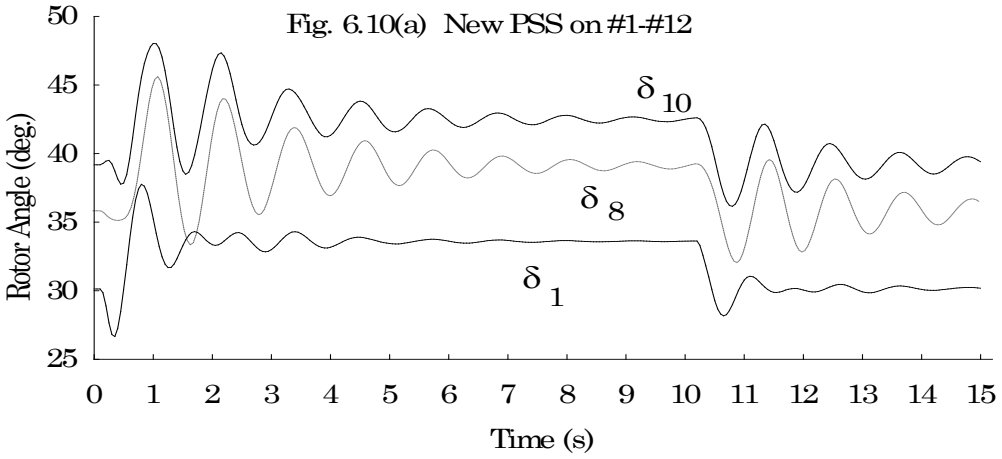

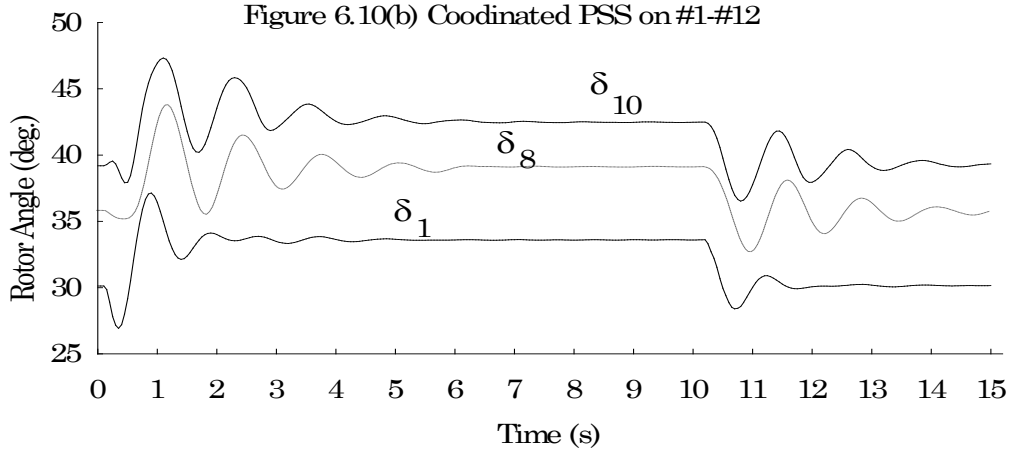

Figure 6.10: Time domain simulations of the SLG fault with new PSSs on all machines in service.

It can be observed that (i) the oscillations using coordinated PSSs take less than half of the time to settle down as compared to that with non-coordinated PSSs (compare Figures 6.9(a) with 6.9(b), 6.10(a) with 6.10(b)), and (ii) coordinated PSSs on generators #1 to #9 are more efficient than non-coordinated PSSs on all generators (compare Figures 6.9(b) with 6.10(a)).

6.5.4 Other Tests

A number of other disturbances were simulated and a summary of the results obtained is presented in this section. All these tests were conducted with new PSSs only on generators #1 through #9. The objective was to make a valid comparison with the existing PSSs and to avoid the difficulties in installing new PSSs on the hydro generators #10-#12.

1. When there is one PSS failure in each of the three coherent groups, simulation of the SLG fault studied above shows that it took the system 12 seconds to completely settle down to a new equilibrium point without PSS coordination and about 7 seconds with PSS coordination.

2. A minimum of one new PSS for each of the three groups is needed to maintain stable operation of the system. This observation is in agreement with that of [25].

3. A three phase fault of the same duration as the SLG fault on the double circuit was simulated. It took the system 5 seconds more time than in the latter case to damp out the oscillations.

4. A three phase fault for a duration of 6 cycles on the line from Island Falls to Lindsay Lake will separate the system into three parts. The parts from Island Falls to the northern end of the system will be lost

after a number of breaker trips. The objective of this simulation was to examine whether the Island Falls plant could be saved after the disturbance. Figure 6.11 shows the swing of speed difference of generator #1 with the existing PSSs and new PSSs in service, respectively.

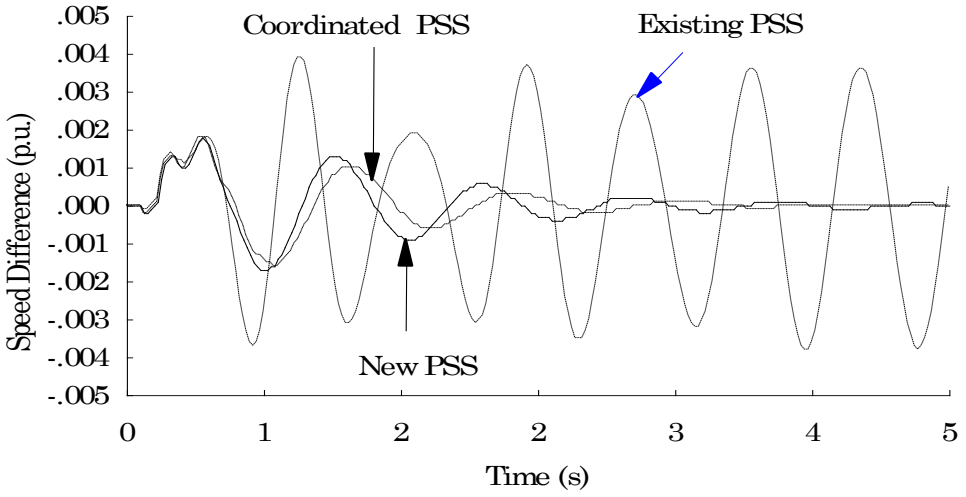

Figure 6.11: Responses of speed difference of generator #1 to 3LG fault for 6 cycles at bus 18.

5. Simulations of the SLG fault for a duration of 6 cycles under 50%, 75% and 100% loading were also performed with coordinated PSSs in service. Figure 6.12 displays the rotor angle swings of generator 1 under different loading. It can be concluded that though the new PSSs were tuned under full system loading, they perform very well under other system loading.

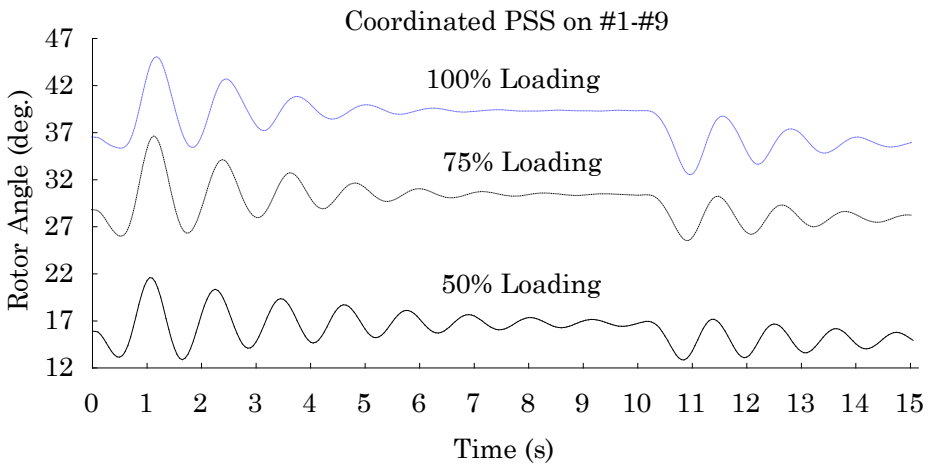

Figure 6.12: Rotor angle swing of generator #1. SLG fault for 6 cycles under different system loading.

6.6 Summary

This chapter presents the effects of the existing primary controls in the APNS. It is shown that the SGTS has little effect on damping and that the existing PSSs do not work as expected. Additional excitation control could be more effective. Secondly, a coordinated design and application procedure for new PSSs is described. New PSSs were designed and their performance is illustrated when they were applied to the system. Finally, a report is given of the results of a comprehensive investigation of the steady state and transient stability of the system.